

Microscopic ensemble bootstrap in phase space

Yu Zhang

*College of Mechanics and Engineering Science,
Hohai University, Nanjing 211100, Jiangsu, China*

(Dated: February 23, 2024)

Abstract

The bootstrap method which has been studied under many quantum mechanical models turns out feasible in microcanonical ensemble as well. While the approach in [Y. Nakayama, Modern Physics Letters A **37**, 10.1142/s0217732322500547 (2022)] produces a sector when energy is negative, in this paper we report a method that has stronger constraints and results in a smaller region. We also study other models to demonstrate the effectiveness of our method.

I. INTRODUCTION

Bootstrap, a novel yet promising method which has been studied in quantum mechanics recently, is a way to utilize the very general self-consistency condition and solve the system numerically. Developed in the 1960s and '70s [1], the method was later applied in large N systems [2–4], lattice theory [5–8], conformal field theory [9–14] as well as matrix models [15, 16]. This technique is also used to bootstrap the Dirac ensembles [17], some have integrated this method with artificial intelligence [18, 19]. And the bootstrap approaches used to find the eigen energies for bound states in recent papers are mostly inspired by Han [20]. Some papers have studied different systems using this method [21–27], and many have reported the accuracy and high precision of the method. In certain cases the bootstrap evolves into Dirac’s ladder operator approach and can be solved analytically, suggesting some underlying mechanism of this method [28]. In this paper, we report an approach that can be seen as a classical correspondence to Han’s.

Although widely studied in quantum mechanics, one can also apply the method to microcanonical ensembles as the fundamental relations of bootstrapping are still applicable and have their classical correspondence (3), (4), and (5) as $\hbar \rightarrow 0$.

Nakayama [29] first introduced this method into the classical scenario, despite reporting the feasibility of the approach, he mentioned a peninsula in $E < 0$ which doesn’t converge even for larger bootstrap matrices in the double-well potential. In this paper, we use a different approach that incorporates more information in phase space and thus exhibiting a much stronger constraint. We will see that the result of the double-well bootstrap in phase space cancels the sector region in $E < 0$ compared to the x only bootstrap.

We also investigate coulomb potential, a harmonic oscillator and a non-relativistic TODA model. The first two can be solved analytically (here by analytically we mean that the

averages of observables can be written in a form of E) via the bootstrap approach which, however, are trivial cases. As for the non-relativistic TODA model, our approach in phase space once again demonstrates a more powerful restriction, maybe overly powerful that we can merely see a few points in the result if the sample isn't large enough. Since Hu [30] has discussed many models and derived lots of bootstrap equations, most of our models are modified versions of his.

Yet a stronger constraint as our approach may have, it still cannot converge to the exact solution in some places, like the non-relativistic TODA model. Not to mention that our approach consumes much more computing power, for the size of our bootstrap matrix is $O(n^4)$. But the benefit is that we can easily achieve high precision when the result converges.

II. MICROCANONICAL ENSEMBLE BOOTSTRAP

A. Bootstrap Equations and Matrices

Starting with the Hamiltonian we have

$$H = \frac{p^2}{2M} + V(x) \quad (1)$$

for microcanonical ensemble the average of an observable $\mathcal{O}(x, p)$ is

$$\langle \mathcal{O}(x, p) \rangle = \frac{\int dx dp \mathcal{O}(x, p) \delta(E - H)}{\int dx dp \delta(E - H)} \quad (2)$$

and we can easily find that

$$\langle \{H, \mathcal{O}\} \rangle = 0 \quad (3)$$

$$\langle H\mathcal{O} \rangle = E \langle \mathcal{O} \rangle \quad (4)$$

here $\{H, \mathcal{O}\}$ is the poisson bracket. As for the positivity constraints, obviously for any observable \mathcal{O} we would have

$$\langle \mathcal{O}^* \mathcal{O} \rangle \geq 0 \quad (5)$$

and by writing the observable as a polynomial of certain observable o , $\mathcal{O} = \sum_{i=0}^k a_i o^i$, one can construct a bootstrap matrix which can be defined as

$$\mathcal{M}_{ij} = \langle (o^*)^i o^j \rangle, \quad i, j = 0, 1, \dots, k \quad (6)$$

we can then rewrite the constraints (5) with matrix and vectors

$$\boldsymbol{\alpha}^\dagger \boldsymbol{\mathcal{M}} \boldsymbol{\alpha} \geq 0 \quad (7)$$

as (7) should hold true for any vector $\boldsymbol{\alpha}$, the bootstrap matrix $\boldsymbol{\mathcal{M}}$ must embody the positive semi definiteness i.e. $\boldsymbol{\mathcal{M}} \succeq 0$, which is essentially an eigenvalue problem

$$\forall (\boldsymbol{\mathcal{M}})_{\text{eigenvalue}} \geq 0 \quad (8)$$

When the observable \mathcal{O} is a coupling of two observables, say, A and B

$$\mathcal{O} = \sum_{i,j=0}^{k-1} a_i b_j A^i B^j \quad (9)$$

$$\mathcal{O}^* \mathcal{O} = \sum_{i_1, j_1, i_2, j_2=0}^{k-1} a_{i_1}^* b_{j_1}^* (B^*)^{j_1} (A^*)^{i_1} A^{i_2} B^{j_2} a_{i_2} b_{j_2} \quad (10)$$

we can define two auxiliary matrices $\boldsymbol{\mathcal{M}}_{ij}^0 = (B^*)^j (A^*)^i$ and $\boldsymbol{\mathcal{M}}_{ij}^1 = A^i B^j$, the constraints may be written as

$$\boldsymbol{\mathcal{M}}_{ij} = \langle (\boldsymbol{\mathcal{M}}^0 \otimes \boldsymbol{\mathcal{M}}^1)_{ij} \rangle, \quad i, j = 0, 1, 2, \dots, k^2 - 1 \quad (11)$$

$$\boldsymbol{\mathcal{M}} \succeq 0 \quad (12)$$

B. Recursion Formula

Taking \mathcal{O} as $x^m p^n$ and substituting Hamiltonian(1) into (3) and (4), we immediately obtain

$$\begin{aligned} n \left\langle \frac{dV}{dx} x^m p^{n-1} \right\rangle &= 2Em \langle x^{m-1} p^{n-1} \rangle - 2m \langle V x^{m-1} p^{n-1} \rangle \\ E \langle x^m p^n \rangle &= \frac{1}{2m} \langle x^m p^{n+2} \rangle + \langle V x^m p^n \rangle \end{aligned} \quad (13)$$

this would do the trick for the potential with polynomial of x . When the potential is in the form of exponentials, we need to take \mathcal{O} as $e^{mx} p^n$

$$\begin{aligned} n \left\langle \frac{dV}{dx} e^{mx} p^{n-1} \right\rangle &= 2Em \langle e^{mx} p^{n-1} \rangle - 2m \langle V e^{mx} p^{n-1} \rangle \\ E \langle e^{mx} p^n \rangle &= \frac{1}{2M} \langle e^{mx} p^{n+2} \rangle + \langle V e^{mx} p^n \rangle \end{aligned} \quad (14)$$

C. Methodology Framework

With the recursion formula(13) or (14) and a few initial values we can construct a whole bootstrap matrix \mathcal{M} , and by testing the positive semi definiteness of the matrix the validity of the initial values can be determined. By doing so over all the possible initial values we will eventually find the allowed regions restricted by positivity constraint.

III. NUMERICAL EXAMPLES

A. Double-Well Potential

The Hamiltonian of a double-well potential can be written as

$$H = p^2 - x^2 + x^4 \quad (15)$$

taking $M = \frac{1}{2}$ and with (13) we have

$$2(2n + m) \langle x^{m+3} p^{n-1} \rangle = 2(m + n) \langle x^{m+1} p^{n-1} \rangle + 2mE \langle x^{m-1} p^{n-1} \rangle \quad (16)$$

$$\langle H x^m p^n \rangle = E \langle x^m p^n \rangle = \langle x^m p^{n+2} \rangle - \langle x^{m+2} p^n \rangle + \langle x^{m+4} p^n \rangle \quad (17)$$

plus $\langle \{H, x^m\} \rangle = 0$, we get

$$\langle x^{m-1} p \rangle = 0 \quad (18)$$

and for simplicity, we here assume that the average of x to the odd powers is 0

$$\langle x^m \rangle = 0, \quad \text{for all odd } m \quad (19)$$

with (16) (17) (18) (19) plus the initial paratemers E and $\langle x^2 \rangle$ we can construct the bootstrap matrix \mathcal{M} . The result when $k = 5$ is shown in Fig. 1. We also reproduced the result in [29] to make a comparison.

In constrast with [29], our result shows no peninsula when E is negative, as we include the information of the momentum. When E turns negative, the curve manifests a similar behavior as the positive part. In our program the scale of the bootstrap matrix is k^4 , which is much larger compared to the single observable bootstrap program with the scale of k^2 . So here the size of our bootstrap matrix is 625, about seven times bigger than that of the x bootstrap. But the region still doesn't shrink even when we set $k = 25$ for the x only bootstrap program, so we conclude that this bootstrap in phase space does have a much stronger constraint than the single observable one.

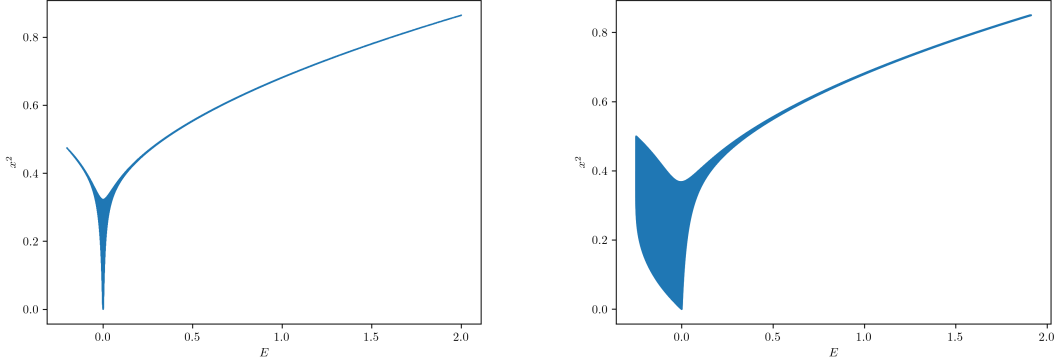


FIG. 1. xp bootstrap with $k = 5$ (left), x only bootstrap with $k = 9$ (right)

B. Harmonic Oscillator and Coulomb Potential

Consider a harmonic oscillator, its Hamiltonian is

$$H = p^2 + x^2 \quad (20)$$

and again, we can obtain the recursion formula

$$\begin{aligned} 2n \langle x^{m+1} p^{n-1} \rangle &= 2Em \langle x^{m-1} p^{n-1} \rangle - 2m \langle x^{m+1} p^{n-1} \rangle \\ E \langle x^m p^n \rangle &= \langle x^m p^{n+2} \rangle + \langle x^{m+2} p^n \rangle \end{aligned} \quad (21)$$

since $\langle x^0 p^0 \rangle = 1$ and $\langle x \rangle = 0$, and (18) also holds true, we only need the initial energy E to bootstrap. The result of bootstrap is shown in Fig.2, as we sample E from negative to positive, we can see that the negative energies are rejected by the bootstrap program. ~~While the x -only bootstrap can also generate the same plot, our approach reaches an accuracy about 100 times higher than the x -only bootstrap, because to obtain the same result, our method requires sampling more than 100 times as many data points as the original one. Also, since our matrix scales at a rate of fourth power, the numerical precision needed in our program also increases rapidly, or else we will see that many valid E s are to be rejected by the xp bootstrap[31].~~

As for the coulomb potential, assume the Hamiltonian

$$H = p^2 - \frac{1}{r} + \frac{1}{r^2} \quad (22)$$

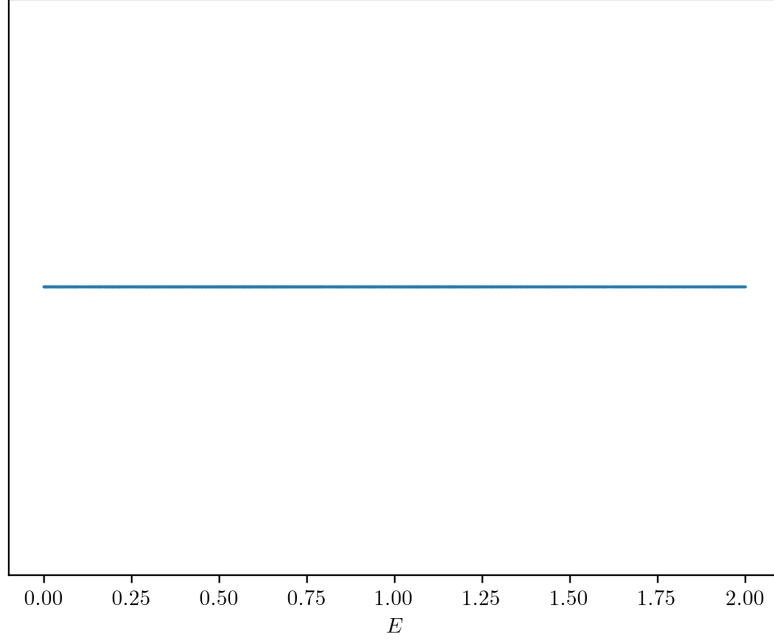


FIG. 2. Allowed regions in xp bootstrap ($k = 4$) for harmonic oscillator

here $-\frac{1}{r} + \frac{1}{r^2}$ is the effective potential. The recursion equations are

$$\begin{aligned} 2mE \langle r^{m-1} p^{n-1} \rangle &= 2(m-n) \langle r^{m-3} p^{n-1} \rangle + (n-2m) \langle r^{m-2} p^{n-1} \rangle \\ E \langle r^m p^n \rangle &= \langle r^m p^{n+2} \rangle - \langle r^{m-1} p^n \rangle + \langle r^{m-2} p^n \rangle \end{aligned} \quad (23)$$

Substituting $m = n = 1$ into the first equation we can get

$$2E = -\langle r^{-1} \rangle \quad (24)$$

which is the Virial theorem. This time we only need E in the x bootstrap, while for the xp bootstrap we also need r^{-2} because at some points the coefficients in formula(23) turn to 0 and thus breaking the recursion. The initial value r^{-2} gives the exact information we need to patch up these points, together with equation (18) the results of bootstrap are shown in Fig3 and Fig4. Here we can see that our xp bootstrap excludes the positive E which will cause the r go negative. But there is some noise around $E \rightarrow 0$, and again this is due to loss of precision[32]. With the equation (18), again we only need E to bootstrap the coulomb potential. The result is shown in Fig3. However, this time we failed to find any points using $x^m p^n$ bootstrap, we speculate that this is due to insufficient numerical precision. But the

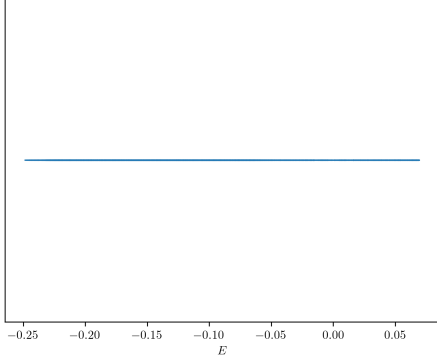


FIG. 3. Allowed regions in $x \langle x^m \rangle$ bootstrap ($k = 8$) for coulomb potential

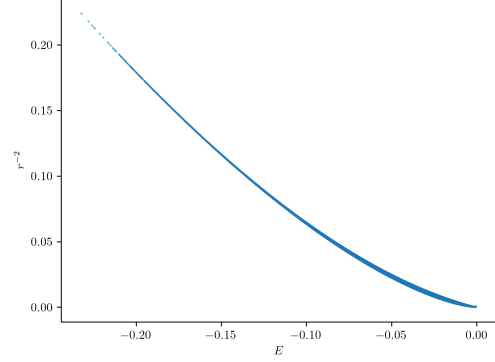


FIG. 4. Allowed regions in xp bootstrap ($k = 3$) for coulomb potential

~~x^m bootstrap is doing great, at least we successfully find the allowed energy.~~

C. Non-Relativistic TODA model

For a non-relativistic TODA model, the Hamiltonian might be written as

$$H = p^2 + e^x + e^{-x} \quad (25)$$

the recursion equations are

$$\begin{aligned} (n + 2m) \langle e^{m+1} p^{n-1} \rangle &= 2E \langle e^m p^{n-1} \rangle + (n - 2m) \langle e^{m-1} p^{n-1} \rangle \\ E \langle e^{mx} p^n \rangle &= \langle e^{mx} p^{n+2} \rangle + \langle e^{(m+1)x} p^n \rangle + \langle e^{(m-1)x} p^n \rangle \end{aligned} \quad (26)$$

and studying $\langle \{H, e^{mx}\} \rangle$ we have

$$\langle e^{(m-1)x} p \rangle = 0 \quad (27)$$

using the initial parameters E and $\langle e^x \rangle$, the bootstrap result is shown in Fig.5

The two observables bootstrap shows a much stronger constraint than the single one, in this non-relativistic TODA mode the e^{mx} bootstrap even fails to reject the negative E , and results in a much larger region. Our approach may have better precision, yet the allowed region still tends to diverge when E goes large in Fig. 6.

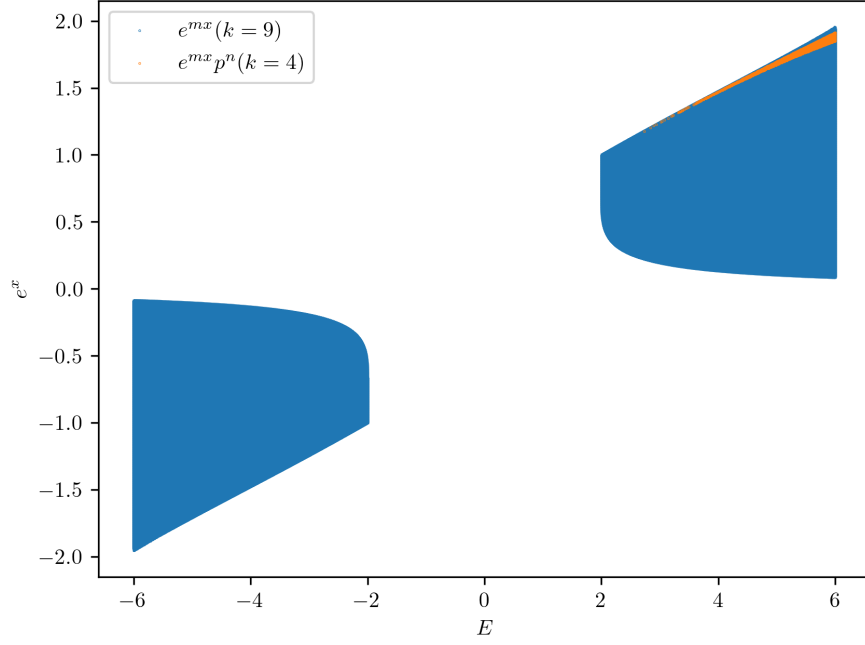


FIG. 5. Allowed regions in xp bootstrap for non-relativistic TODA model

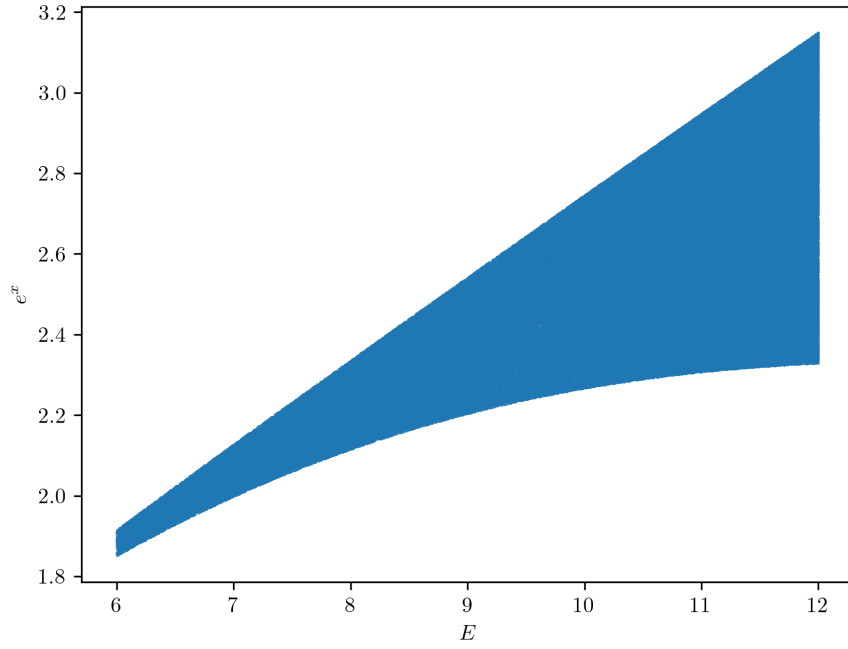


FIG. 6. Allowed region diverges as E grows

IV. CONCLUSIONS

In this paper, we study two different bootstrap approaches in various models, our approach outperforms the single observable bootstrap program in most cases. ~~in some models e.g. double-well, non-relativistic TODA model, while in other two models our bootstrap in phase space fails to achieve a satisfactory result, the single observable one already restricts the model pretty well.~~ We've seen that it cancels the sector region in double well potential, excludes some invalid E s in both harmonic oscillator and non-relativistic TODA model. Although it performs better and achieves a much higher precision, it still fails to converge to the exact solution, and even tends to diverge. Like in the situations that $E \rightarrow 0$ in the double-well potential, $E \rightarrow \infty$ in the non-relativistic TODA model, we might still be missing some information to pin point the final answer.

ACKNOWLEDGEMENTS

I would like to thank Dong Bai for discussions and encouragements. I would also like to acknowledge Zhaobin Huang for reading the manuscript and valuable comments.

-
- [1] Wikipedia contributors, Bootstrap model — Wikipedia, the free encyclopedia, https://en.wikipedia.org/w/index.php?title=Bootstrap_model&oldid=1195984682 (2024), [Online; accessed 28-January-2024].
 - [2] A. Jevicki, O. Karim, J. Rodrigues, and H. Levine, Loop space hamiltonians and numerical methods for large-n gauge theories, Nuclear Physics B **213**, 169 (1983).
 - [3] A. Jevicki, O. Karim, J. Rodrigues, and H. Levine, Loop-space hamiltonians and numerical methods for large-n gauge theories (ii), Nuclear Physics B **230**, 299 (1984).
 - [4] J. P. Rodrigues, Numerical solution of lattice schwinger-dyson equations in the large-n limit, Nuclear Physics B **260**, 350 (1985).
 - [5] P. D. Anderson and M. Kruczenski, Loop equations and bootstrap methods in the lattice, Nuclear Physics B **921**, 702 (2017).
 - [6] S. Lawrence, Bootstrapping lattice vacua (2021), arXiv:2111.13007 [hep-lat].

- [7] V. Kazakov and Z. Zheng, Bootstrap for lattice yang-mills theory, *Physical Review D* **107** (2023).
- [8] Anderson, Peter and Kruczenski, Martin, Loop equation in lattice gauge theories and bootstrap methods, *EPJ Web Conf.* **175**, 11011 (2018).
- [9] D. Poland, S. Rychkov, and A. Vichi, The conformal bootstrap: Theory, numerical techniques, and applications, *Rev. Mod. Phys.* **91**, 015002 (2019).
- [10] A. Guerrieri, J. a. Penedones, and P. Vieira, Where is string theory in the space of scattering amplitudes?, *Phys. Rev. Lett.* **127**, 081601 (2021).
- [11] S. El-Showk, M. F. Paulos, D. Poland, S. Rychkov, D. Simmons-Duffin, and A. Vichi, Solving the 3d ising model with the conformal bootstrap, *Phys. Rev. D* **86**, 025022 (2012).
- [12] S. El-Showk, M. F. Paulos, D. Poland, S. Rychkov, D. Simmons-Duffin, and A. Vichi, Solving the 3d ising model with the conformal bootstrap, *Physical Review D* **86** (2012).
- [13] S. El-Showk, M. F. Paulos, D. Poland, S. Rychkov, D. Simmons-Duffin, and A. Vichi, Solving the 3d ising model with the conformal bootstrap ii. c -minimization and precise critical exponents, *Journal of Statistical Physics* **157**, 869–914 (2014).
- [14] D. Simmons-Duffin, The lightcone bootstrap and the spectrum of the 3d ising cft, *Journal of High Energy Physics* **2017** (2017).
- [15] H. W. Lin, Bootstraps to strings: solving random matrix models with positivity, *Journal of High Energy Physics* **2020** (2020).
- [16] V. Kazakov and Z. Zheng, Analytic and numerical bootstrap for one-matrix model and “unsolvable” two-matrix model, *Journal of High Energy Physics* **2022** (2022).
- [17] H. Hessam, M. Khalkhali, and N. Pagliaroli, Bootstrapping dirac ensembles, *Journal of Physics A: Mathematical and Theoretical* **55**, 335204 (2022).
- [18] G. Kántor, V. Niarchos, and C. Papageorgakis, Conformal bootstrap with reinforcement learning, *Physical Review D* **105** (2022).
- [19] G. Kántor, C. Papageorgakis, and V. Niarchos, Solving conformal field theories with artificial intelligence, *Physical Review Letters* **128** (2022).
- [20] X. Han, S. A. Hartnoll, and J. Kruthoff, Bootstrapping matrix quantum mechanics, *Physical Review Letters* **125** (2020).
- [21] J. Bhattacharya, D. Das, S. K. Das, A. K. Jha, and M. Kundu, Numerical bootstrap in quantum mechanics, *Phys. Lett. B* **823**, 136785 (2021), arXiv:2108.11416 [hep-th].

- [22] D. Berenstein and G. Hulsey, Bootstrapping more QM systems, *J. Phys. A* **55**, 275304 (2022), arXiv:2109.06251 [hep-th].
- [23] B.-n. Du, M.-x. Huang, and P.-x. Zeng, Bootstrapping Calabi–Yau quantum mechanics, *Commun. Theor. Phys.* **74**, 095801 (2022), arXiv:2111.08442 [hep-th].
- [24] Y. Aikawa, T. Morita, and K. Yoshimura, *Physical Review D* **105** (2022).
- [25] S. Tchoumakov and S. Florens, Bootstrapping bloch bands, *Journal of Physics A: Mathematical and Theoretical* **55**, 015203 (2021).
- [26] D. Bai, Bootstrapping the deuteron (2022), arXiv:2201.00551 [nucl-th].
- [27] D. Berenstein and G. Hulsey, Bootstrapping simple qm systems (2021), arXiv:2108.08757 [hep-th].
- [28] Y. Aikawa, T. Morita, and K. Yoshimura, Bootstrap method in harmonic oscillator, *Phys. Lett. B* **833**, 137305 (2022), arXiv:2109.08033 [hep-th].
- [29] Y. Nakayama, Bootstrapping microcanonical ensemble in classical system, *Modern Physics Letters A* **37** (2022).
- [30] X. Hu, Different Bootstrap Matrices in Many QM Systems (2022), arXiv:2206.00767 [quant-ph].
- [31] For more details go to the appendix.
- [32] For more details go to the appendix.